

# Electrochemical Characteristics of Nickel Hydroxide Fabricated from a Spent Electroless Plating Bath

Tzu-Hsuan Tsai<sup>1</sup>, Hao-Wei Chou<sup>1</sup>, Yung-Fu Wu<sup>2,\*</sup>

<sup>1</sup> Department of Materials and Mineral Resources Engineering, National Taipei University of Technology, Taipei 10608, Taiwan

<sup>2</sup> Department of Chemical Engineering, Ming Chi University of Technology, New Taipei City 24301, Taiwan

\*E-mail: [gausswu@mail.mcut.edu.tw](mailto:gausswu@mail.mcut.edu.tw)

Received: 11 October 2021 / Accepted: 17 November 2021 / Published: 5 January 2022

---

Electroless nickel plating baths must be replaced periodically to retain the quality of the deposited nickel film, thus resulting in a considerable amount of spent plating solution. In the spent plating solution, Ni<sup>2+</sup> of sufficiently high concentration can be reused for energy storage applications. This study investigated a chemical precipitation method that involved adding sodium hydroxide and polyethylene glycol to generate 0.5- $\mu\text{m}$  Ni(OH)<sub>2</sub> particles. The electrochemical experimental results indicated that an electrode consisting of Ni(OH)<sub>2</sub> and Vulcan XC72 carbon black could provide active sites for charge storage because of the layered structure of the Ni(OH)<sub>2</sub>. The interstitial water between the layers enhanced the transport of H<sup>+</sup> with a diffusivity of  $1.4 \times 10^{-12}$  cm<sup>2</sup>/s, which was twice as high as that of an electrode made from commercial Ni(OH)<sub>2</sub>. Furthermore, a charging-discharging measurement with 100 cycles revealed that the electrode made with Ni(OH)<sub>2</sub> from a spent plating bath exhibited 88% capacitance retention, which was greater than that of the electrode made from the commercial Ni(OH)<sub>2</sub>. Consequently, the method proposed in this study may provide usable materials for energy storage while removing nickel from spent plating baths.

---

**Keywords:** Nickel hydroxide, electroless plating bath, precipitation, energy storage

## 1. INTRODUCTION

Management of the spent solution of electroless nickel plating is of worldwide concern because of the widespread industrial use of plating for enhancing brightness, wear resistance, and corrosion protection [1]. To maintain the performance of electroless nickel plating, frequent replacement of the plating bath is necessary [2]. Generally, the spent bath still contains 85% of the initial amount of nickel. A study on the wastewater reported that 62% of nickel in wastewater originates from the plating industry

[3]. Furthermore, epidemiological studies have revealed that nickel is toxic and carcinogenic [4, 5]. Therefore, the discharge of the spent bath not only negatively affects an impact on the environment, but also leads to an enormous loss of metal resources.

A typical electroless nickel plating bath consists of a nickel salt, a reducing agent, a complexing agent, and a pH buffer agent [1]. Ammonia is a commonly used complexing agent and prevents the reduction of nickel, leading to an alkaline environment. Hypophosphite ( $\text{H}_2\text{PO}_2^-$ ) is the most effective reducing agent for nickel plating. However, the phosphorous product included in the spent bath also causes water pollution by enhancing algae growth [2]. Because the combination of nickel ions, ammonia, and hypophosphite effectively stabilizes a spent plating bath, the treatment of wastewater or recovery of valuable components is challenging.

To date, numerous treatments have been proposed to maximize the utility of and minimize the damage caused by spent baths containing a considerable amount of nickel. The underlying goals of these treatments are the removal of impurities for reuse in plating and the recovery of nickel before drainage. Nickel in the spent bath can be separated through electrochemical reduction, chemical precipitation, ion exchange, or adsorption [3–16]. Among these methods, chemical precipitation is used most often because of its low cost, but a large amount of sludge typically formed after the procedure. This sludge is mainly composed of  $\text{Ni}(\text{OH})_2$  [5].  $\text{Ni}(\text{OH})_2$  has been widely used as the active material in nickel-based batteries [17], electrochemical capacitors [18–23], and electrochemical sensors [24, 25]. Therefore, a low-cost and ecofriendly method for obtaining  $\text{Ni}(\text{OH})_2$  from a spent plating bath through by chemical precipitation was investigated in this study.

$\text{Ni}(\text{OH})_2$  precipitates are generated in solutions containing nickel salts and alkali compounds. Chang et al. [26] and Li et al. [27, 28] mixed  $\text{NiSO}_4$  and  $\text{NaOH}$  at a pH of 10–11 and a temperature of 50–60°C to obtain  $\text{Ni}(\text{OH})_2$ . Shrueth et al. used  $\text{NiSO}_4$  and  $\text{KOH}$  to produce  $\text{Ni}(\text{OH})_2$  [29]. Zhang et al. added  $\text{NaOH}$  to a solution containing  $\text{NiSO}_4$  and  $\text{NH}_3$  to prepare micro-sized  $\text{Ni}(\text{OH})_2$  for application in Ni–MH batteries [30]. Miao et al. studied the electrochemical performance of  $\text{Ni}(\text{OH})_2$  made from  $\text{Ni}(\text{NO}_3)_2$ ,  $\text{Ca}(\text{NO}_3)_2$ , and  $\text{Na}_3\text{PO}_4$  at a pH of 9 [31]. Wang et al. added sodium citrate and  $\text{NaBH}_4$  to a solution containing  $\text{Ni}^{2+}$  and mixed in  $\text{NaOH}$  to obtain small-sized  $\text{Ni}(\text{OH})_2$  [32]. Thus, micro-sized or nano-sized precipitates can be obtained through the addition of reducing and complexing agents to a solution containing  $\text{Ni}^{2+}$ . Spent plating baths thus representing a suitable reaction environment for the production of small-sized  $\text{Ni}(\text{OH})_2$ , which is valuable for use in energy storage devices. However, few studies have explored the recovery of small-sized  $\text{Ni}(\text{OH})_2$  directly from spent plating baths.

The aim of this study, therefore, is to examine the characteristics of  $\text{Ni}(\text{OH})_2$  obtained from a spent plating solution and analyze the electrochemical behaviors of the recovered  $\text{Ni}(\text{OH})_2$  using cyclic voltammetry (CV). Furthermore, the capacitor effect of an electrode made from  $\text{Ni}(\text{OH})_2$  was investigated to verify the feasibility of using waste to create energy storage materials.

## 2. EXPERIMENTAL METHOD

### 2.1. Composition of the Spent Nickel Plating Solution

The spent electroless nickel plating solution employed in this study was acquired from Global Wafers. The pH and conductivity of the solution were measured using a pH meter (S-2200, SUNTEX) and an electrical conductivity meter (Cond 720, WTW). The main components of the spent solution include  $\text{Ni}^{2+}$ ,  $\text{NH}_3$ ,  $\text{H}_2\text{PO}_2^-$ ,  $\text{H}_2\text{PO}_3^-$ , and  $\text{Cl}^-$ . The amount of  $\text{Ni}^{2+}$  was analyzed using an inductively coupled plasma/optical emission spectrometer (ICP/OES, Thermo Scientific iCAP 7000 Series). The concentration of  $\text{Cl}^-$ ,  $\text{H}_2\text{PO}_2^-$ , and  $\text{H}_2\text{PO}_3^-$  were measured using ion chromatography (IC, Metrohm 883 Basic IC Plus). In addition, an ammonium ion-selective electrode (Beckman Model 511142) was used to detect the amount of  $\text{NH}_3$ .

### 2.2. Preparation and Characterization of $\text{Ni}(\text{OH})_2$ Powder

$\text{Ni}(\text{OH})_2$  was generated using chemical precipitation, which involved the addition of 3 M NaOH into the spent solution:



During the precipitation, the pH and temperature of the solution were fixed, and the process duration and stirring speed were controlled. After the reaction was complete, the solution was centrifuged at 10,000 rpm for 15 min. Subsequently, the ICP/OES was used to estimate the residual nickel content. The deposit at the bottom of the centrifuge tube was collected and ultrasonically mixed with 2 mL 95 vol.%  $\text{C}_2\text{H}_5\text{OH}$  and 1 mL deionized water. The wet product was then dried in an oven at  $80^\circ\text{C}$  for 24 h to remove the solvent. Finally, the obtained  $\text{Ni}(\text{OH})_2$  powder was analyzed using a laser diffraction particle size analyzer (LA-300, HORIBA) to determine the particle size distribution.

### 2.3. Preparation and Characterization of $\text{Ni}(\text{OH})_2$ Electrode

To construct the working electrode, an ink was made with containing 10 mg of  $\text{Ni}(\text{OH})_2$ , 1 mg of Vulcan XC72 carbon black (CB), 1 mg of carboxymethyl cellulose (CMC), 3 mL 95 vol.% ethanol, and 7 mL of deionized water. The ink was coated on the surface of a carbon glass electrode with 5 mm in diameter. After baking at  $80^\circ\text{C}$  for 5 min, the electrode was immersed into a 5wt.% Nafion solution, and dried again at  $80^\circ\text{C}$  for 5 min. In the electrochemical analysis system, a platinum plate was used as the counter electrode, a commercial Ag/AgCl electrode (MF-2052, Basi) was used as the reference electrode, and a 2 M KOH solution was used as the electrolyte. The cyclic voltammetry (CV) was performed using a potentiostat (PGSTAT30, Metrohm) to measure the cyclic charging and discharging characteristics. The potential window was set from 0.0 to 0.5 V versus Ag/AgCl electrode. The potential scan rate was adjusted from 2 to 100 mV/s.

### 3. RESULTS AND DISCUSSION

The content of the spent electroless nickel plating solution was analyzed. The analytical results indicated that the spent solution was composed of nickel, hypophosphite, phosphite, chloride, and ammonium ions. Only approximately 12% of the original nickel in the solution was consumed before the plating bath was changed, which reveals that the spent solution was still a rich source of nickel. However, the presence of  $\text{Cl}^-$  and  $\text{NH}_3$  hampers the nickel removal or recovery, because these components chelate nickel ions to stabilize the plating bath.

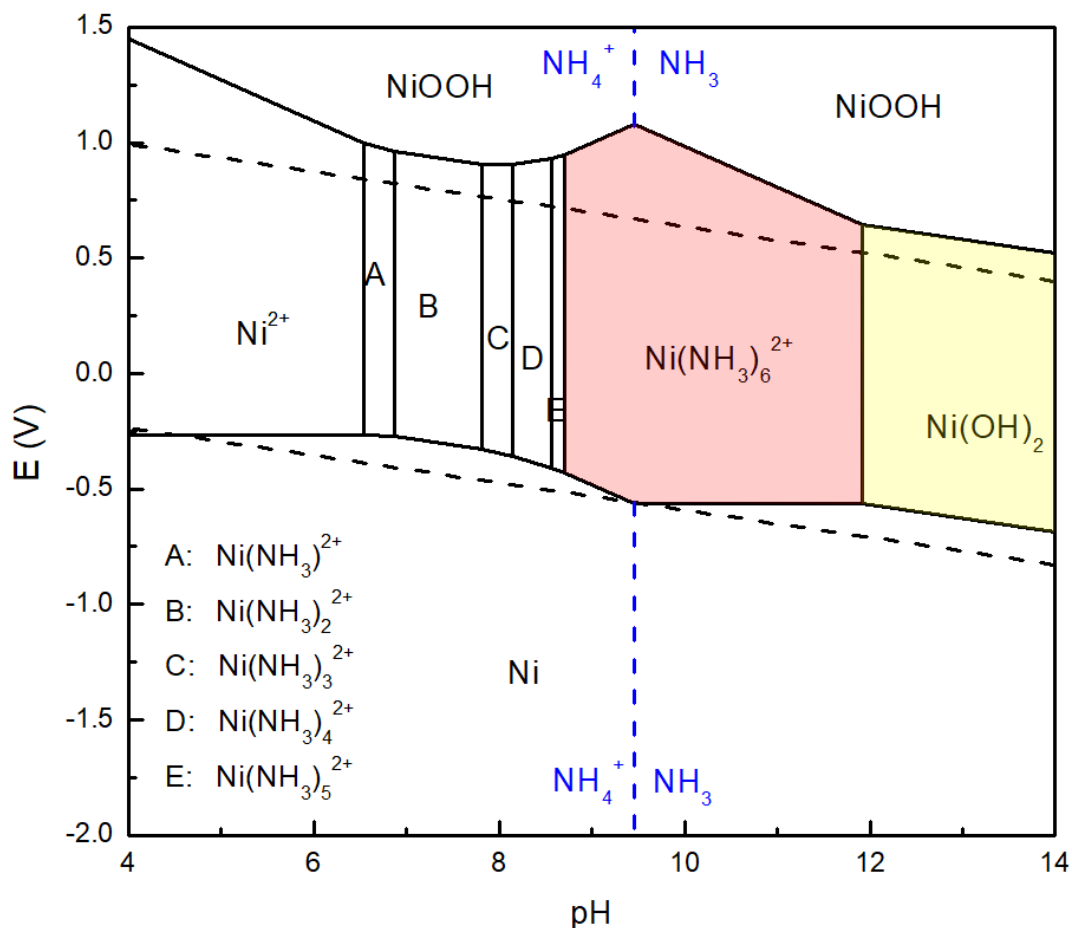


**Figure 1.** E-pH diagram of the Ni system at 25°C. (The total activities of Ni and  $\text{NH}_3$  are 0.116 and 1.000, respectively.  $\text{NH}_3$  is thermodynamically stable at a pH > 9.4.)

To predict the feasibility of nickel recovery from a spent plating solution, the E-pH diagrams of Ni were constructed using HSC 10.0 software (Fig. 1). According to the composition of the spent solution, the total activity of nickel was set to 0.116, and that of ammonia to 1. Generally, a precipitate of  $\text{Ni(OH)}_2$  can be formed when the pH of the solution is more than 7. However,  $\text{Ni(OH)}_2$  is difficult to generate when the solution contains  $\text{NH}_3$  at a pH < 12.  $\text{NH}_3$  can chelate  $\text{Ni}^{2+}$  at a neutral pH, and thus extends the shelf life of plating baths. To remove nickel from a spent plating solution, increasing the pH of the solution and then producing the precipitate may be feasible.

**Table 1.** Solution color change with pH adjusted by NaOH

pH	8.36	10	11	12	13
Plating Solution before precipitation					
Plating Solution after precipitation					

The pH of the spent plating solution was 8.4.  $\text{NH}_3$  in the solution prevents the formation of  $\text{Ni}(\text{OH})_2$  despite the concentration of  $\text{Ni}^{2+}$  being sufficient. However,  $\text{Ni}(\text{OH})_2$  precipitate could be readily generated after NaOH was added. Table 1 displays the color change from the as-received spent solution to the NaOH-treated spent solution. The received spent solution was cyan, while the NaOH-treated spent solution was nearly colorless. This color change reflects the removal of nickel from the spent solution.

Through a series of centrifugation, separation and drying processes, the  $\text{Ni}(\text{OH})_2$  precipitate was collected. The results of the particle size measurements are presented in Fig. 2. Although the chelation of  $\text{NH}_3$  was replaced by the bond formation between Ni and OH when a sufficient amount of NaOH was added,  $\text{NH}_3$  still acted as an inhibitor to the nucleation of  $\text{Ni}(\text{OH})_2$  particles. Therefore, the average size of the obtained particles was approximately  $8.0 \mu\text{m}$ , which is smaller than the size of the particles in the solution without  $\text{NH}_3$ . Considering the potential electrochemical applications, for example, electrode fabrication for batteries or capacitors, the particle size should be reduced to approximately 100 nm. In this study, polyethylene glycol (PEG) with a molecular weight 400 g/mol was added to the spent plating solution. PEG further hindered the growth of the precipitate, thereby limiting the size of the  $\text{Ni}(\text{OH})_2$  particles. As illustrated in Fig. 2, the size distribution for  $\text{Ni}(\text{OH})_2$  particles in the solution containing PEG peaks at approximately  $0.5 \mu\text{m}$ , indicating that the solution meets the particle size requirement for electrochemical applications.

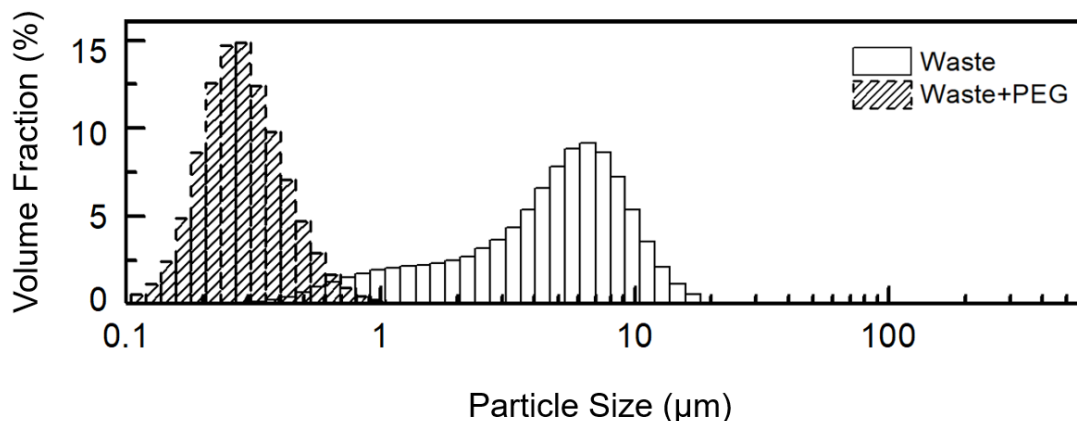


**Figure 2.** Particle size distribution for Ni(OH)<sub>2</sub> generated from the waste plating bath with and without addition of PEG at a stirring speed of 600 rpm.

Figure 3 shows the CV results for the electrode made from the Ni(OH)<sub>2</sub>. The mass ratio of Ni(OH)<sub>2</sub> to CB was 10:1 in 2 M KOH. Figure 3 also illustrates a control curve for the electrode containing only CB, which exhibits no peaks between 0 and 0.5 V vs. Ag/AgCl. However, the electrode with Ni(OH)<sub>2</sub> exhibits a clear oxidative current peak and a capacitor effect in the forward scan range from 0.38 to 0.50 V. Furthermore, the CV curve exhibits a reductive peak in the reverse scan. The potential difference between the oxidative and reductive peaks was 0.067 V, which reveals that the electrochemical reaction that occurred in the electrode with Ni(OH)<sub>2</sub> was somewhat reversible. A possible reaction is described as follows:

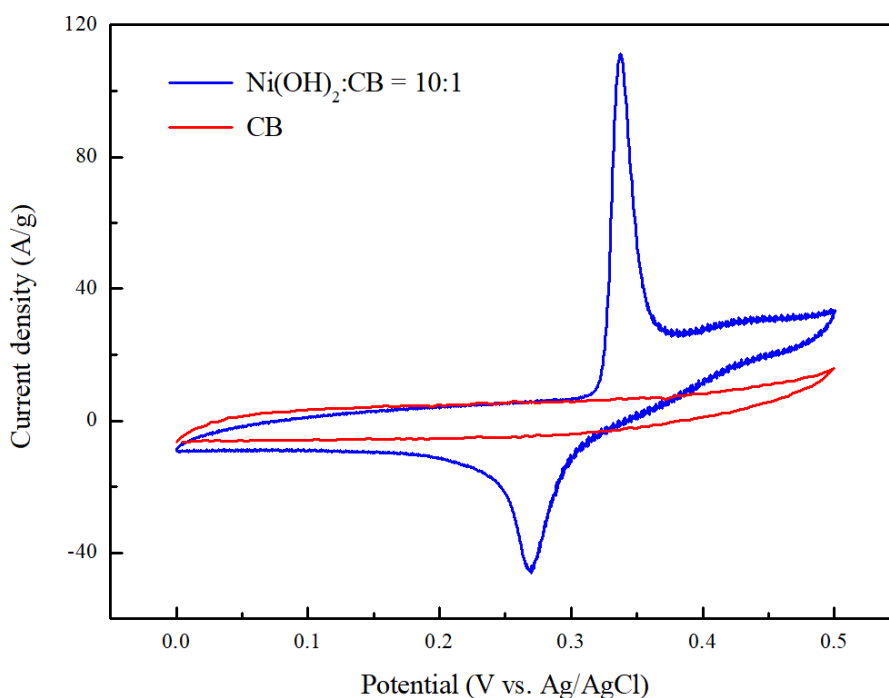
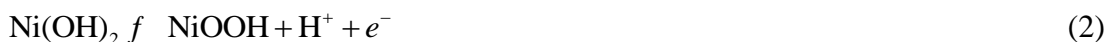


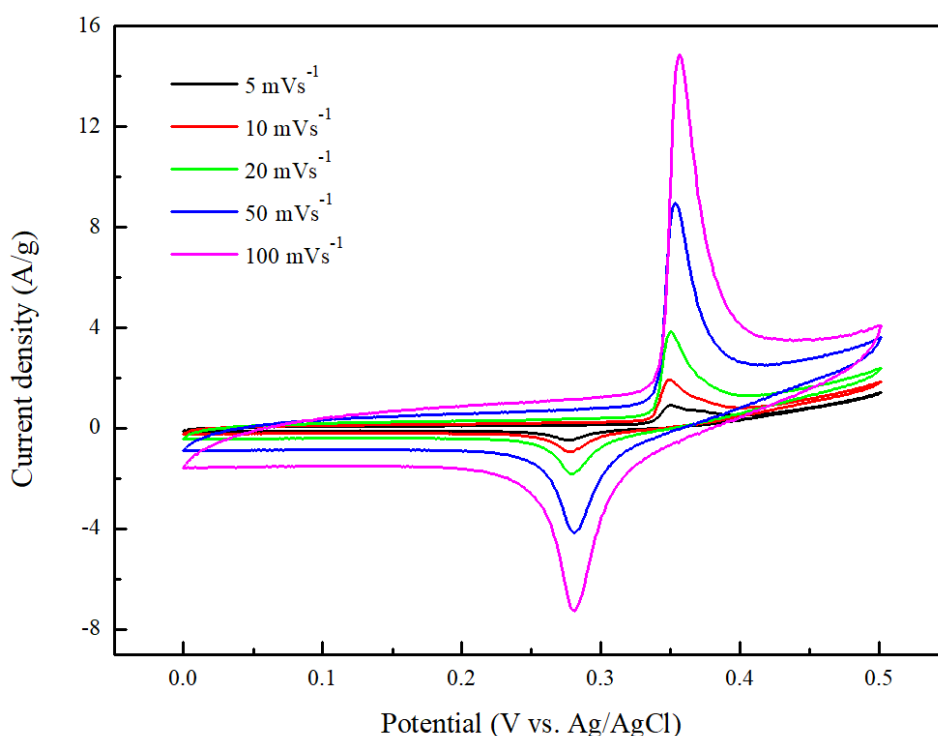
**Figure 3.** Cyclic voltammograms of the electrode coated with Ni(OH)<sub>2</sub> and CB at a mass ratio of 10:1 and the electrode coated with only CB. (The scan rate is 100 mV/s, and the potential window ranges from 0 to 0.50 V.)

The standard potential of the aforementioned oxidative reaction is 1.32 V, but according to the Nernst equation, the electrode potential would shift to 0.4 V in a solution with 2 M KOH at room temperature. The potential at the oxidative peak of the CV curve was approximately 0.35 V, which is consistent with the theoretical prediction. Furthermore, the current peak indicates a mass transfer limitation occurring near the working electrode; therefore,  $H^+$  transport may be inferred to be influenced by the structure of  $Ni(OH)_2$ . Because  $Ni(OH)_2$  is a layered material, the spacing between layers and constituents in the interstices affect the transport of electroactive species. The transport performance can be estimated using the diffusivity of the electroactive species, and the CV measurements can be used to calculate the diffusivity. The theory of CV indicates that the peak current  $I_p$  should be proportional to the square root of the scan rate:

$$I_p = kn^{3/2}AD^{1/2}c\nu^{1/2} \quad (3)$$

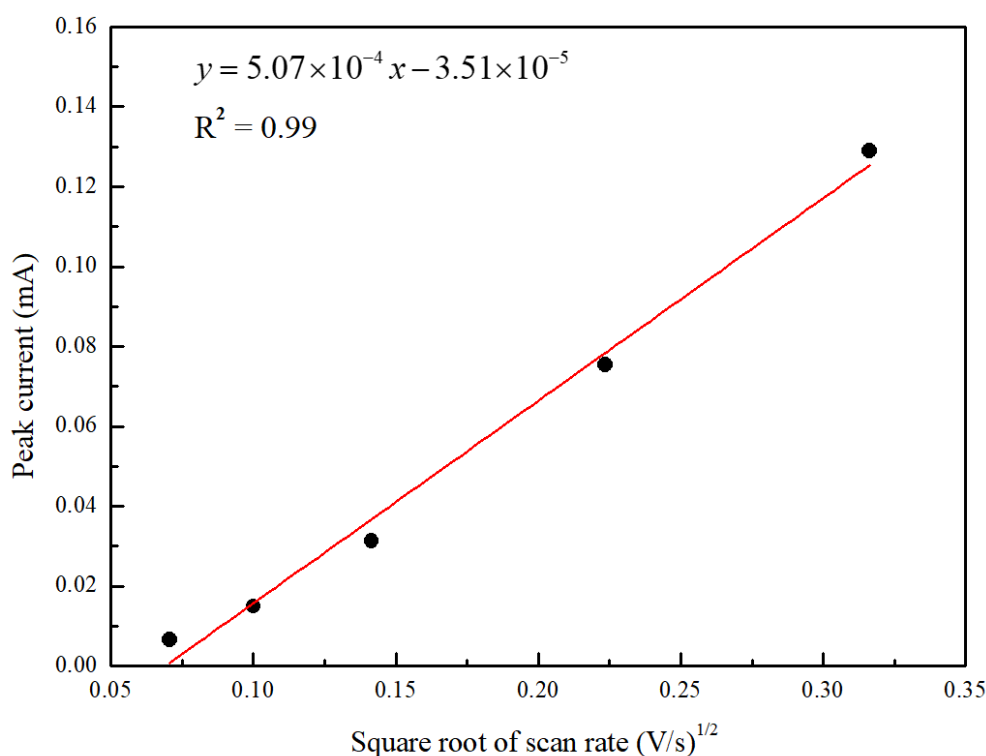
where  $n$  is the number of transferred electrons;  $A$  is the surface area of the electrode;  $D$  and  $c$  are the diffusivity and concentration of  $H^+$ , respectively;  $\nu$  is the potential scan rate; and  $k$  is a constant.

Figure 4 illustrates a series of CV measurements at various scan rates. These curves illustrate the sufficiently high current densities in the potential window beyond the peak potential (i.e., from 0.4 V to 0.5 V). The  $Ni(OH)_2$  structure exhibited a high energy storage capacity most likely because of its wide layer spacing. As shown, the anodic and cathodic peak potentials were consistent with those published for the oxidation of  $Ni(OH)_2$  and the reduction of  $NiOOH$ , respectively [33, 34]. In addition, the electrochemical responses in Fig. 4 exhibit a battery-like current-voltage relationship [35].



**Figure 4.** Cyclic voltammograms of the electrodes coated with  $Ni(OH)_2$  and CB at a mass ratio of 10:1 at various potential scan rates from 5 to 100 mV/s. (The potential window ranges from 0 to 0.50 V.)

According to Eq. (3), when the corresponding CV analysis was conducted at various scan rates, a linear relationship existed between  $I_p$  and  $\nu^{1/2}$ , as illustrated in Figure 5. The linear slope of  $I_p$  versus  $\nu^{1/2}$  can be used to calculate the diffusivity of  $H^+$  in  $Ni(OH)_2$ . The diffusivity of  $H^+$  obtained in our study was  $1.4 \times 10^{-12} \text{ cm}^2/\text{s}$ , approximately twice as high as that of the control sample made of commercial  $Ni(OH)_2$ . The order of the diffusivity is the same as that published by Shruthi et al.,  $3.21 \times 10^{-12} \text{ cm}^2/\text{s}$  [36]. The minor difference might come from the film resistance due to the thickness. X-ray powder diffraction revealed that the  $Ni(OH)_2$  produced in our study was composed of amorphous material,  $\alpha$ -phase material, and interstitial water. The interstitial water can expand the layer spacing and provide a path for the  $H^+$  transport because of its hydrogen bond network. Therefore, the  $Ni(OH)_2$  produced in our study exhibited greater electrochemical behavior than did the control sample.



**Figure 5.** Anodic peak currents in cyclic voltammograms of the electrodes coated with  $Ni(OH)_2$  and CB at various potential scan rates from 5 to 100 mV/s. (The potential window ranges from 0 to 0.50 V.)

The properties of cyclic charging and discharging of the proposed  $Ni(OH)_2$  electrode in 2 M KOH solution was also investigated. Figure 6 illustrates CV curves at the 2nd, 50th, and 100th cycles. As the cycle number increased, the oxidative and reductive peak current densities decreased slightly, whereas the potential difference between two peaks increased slightly. This indicates that the electrochemical reaction that occurred in the electrode with  $Ni(OH)_2$  became less reversible with more potential scans, which is inevitable for an electrochemical device. In this study, the second cycle of

potential scan was selected as the basis for estimating the capacitor effect. The specific capacitance ( $C_{sp}$ ) of the electrode with Ni(OH)<sub>2</sub> is calculated as follows:

$$C_{sp} = \frac{1}{mv(E_c - E_a)} \int_{E_a}^{E_c} IdE \quad (4)$$

where the capacitor effect is estimated from the CV curves between  $E_c = 0$  V and  $E_a = 0.5$  V,  $m$  is the mass of Ni(OH)<sub>2</sub> in the electrode, and  $v$  is the potential scan rate. At 50 mV/s, the  $C_{sp}$  of the Ni(OH)<sub>2</sub> electrode was 540 F/g, whereas that of the control sample was 272 F/g. At 5 mV/s, their  $C_{sp}$  values reached 1187 F/g and 675 F/g, respectively. Kovalenko and Kotok used electrochemical synthesis to produce Ni(OH)<sub>2</sub> and made an electrode. The peak current density of their electrode was 3.7–3.9 A/g at 1 mV/s, and the current changed obviously with increasing cycles [37]. When they used precipitation method to produce Ni(OH)<sub>2</sub>, the  $C_{sp}$  was around 80 F/g at 1 mV/s [38]. In this study, the peak current density and  $C_{sp}$  of the Ni(OH)<sub>2</sub> electrode were as 7 times high as that measured by Kovalenko and Kotok, because a faster scan rate, 50 mV/s, was used. Consequently, these results indicate that our proposed method serves as a low-cost, environmentally friendly, and production-feasible means of fabricating Ni(OH)<sub>2</sub> electrodes for energy storage.

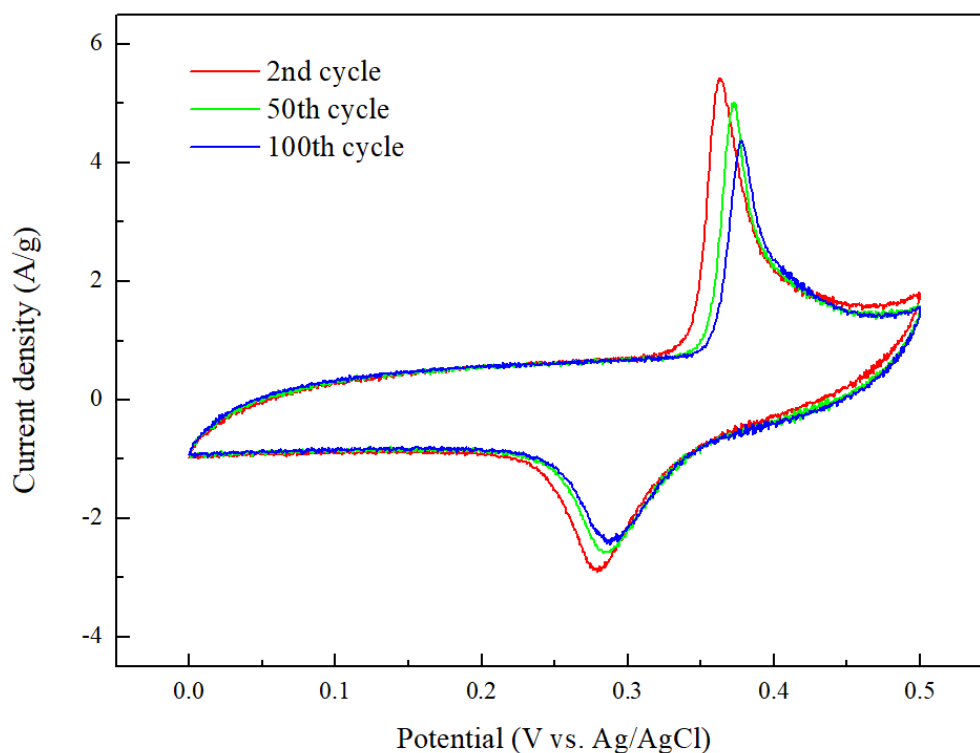


**Figure 6.** Cyclic voltammograms of the electrodes coated with Ni(OH)<sub>2</sub> and CB at the 2nd, 50th and 100th cycles. (The potential scan rate is set at 50 mV/s. The potential window ranges from 0 to 0.50 V.)

To examine the durability of the proposed Ni(OH)<sub>2</sub> electrode for energy storage, the capacitance retention effect was measured. The retention percentage is defined as the ratio of the  $C_{sp}$  at each cycle to

that at the second cycle. The results indicate that the retention percentage of the proposed Ni(OH)<sub>2</sub> electrode was 88% at the 100th scan, whereas that of the control sample was 86%. This decrease in the retention percentage may be attributed to bubble adsorption. The charging and discharging processes cause the evolution of O<sub>2</sub> or H<sub>2</sub>, and the adsorption of bubbles might occupy active sites on the Ni(OH)<sub>2</sub> surface. Furthermore, gas bubbles reduce the contact conductivity between active particles, also causing a decrease in capacitance. The proposed Ni(OH)<sub>2</sub> electrode, however, still exhibited greater cyclic durability than did the commercial sample. Thus, our results indicate that the proposed precipitation method may be used to provide usable materials for energy storage and remove nickel from spent plating solutions.

#### 4. CONCLUSIONS

Electroless nickel plating is widely used in diverse fields. However, the plating bath must be replaced periodically to retain the quality of the deposited film, resulting in a considerable amount of spent plating solution being generated and requiring treatment. In the spent plating solution, Ni<sup>2+</sup> is present in sufficient concentration for reuse in other applications. In our study, chemical precipitation involving the addition of NaOH was adopted to generate 0.5- $\mu\text{m}$  Ni(OH)<sub>2</sub> particles that can be applied to fabricate an electrode for a capacitor. The results indicate that electrodes consisting of Ni(OH)<sub>2</sub> and Vulcan XC72 CB can provide active sites for charge storage because of the layered structure of Ni(OH)<sub>2</sub>. Because the interstitial water between the layers enhanced the transport of H<sup>+</sup>, electrodes made from the precipitated Ni(OH)<sub>2</sub> exhibited a higher current density than did electrodes made from the commercial Ni(OH)<sub>2</sub>. Furthermore, the charging–discharging measurement at 100 cycles revealed that the electrode made with Ni(OH)<sub>2</sub> from a spent plating bath was more durable than that made from the commercial Ni(OH)<sub>2</sub>. Therefore, usable materials for energy storage may be obtained through the precipitation of spent plating baths.

#### ACKNOWLEDGEMENTS

The authors would like to thank the Ministry of Science and Technology in Taiwan for financially supporting this research.

#### References

1. F. Delaunois, V. Vitry, L. Bonin, *Electroless Nickel Plating: Fundamentals to Applications*, 1st ed., Boca Raton, CRC Press, 2019.
2. P. Liu, C. Li, X. Liang, G. Lu, J. Xu, X. Dong, W. Zhang, F. Ji, *Green Chem.*, 16 (2014) 1217–1224.
3. D. Guillard, A. E. Lewis, *Ind. Eng. Chem. Res.*, 40 (2001) 5564–5569.
4. A. Frances, M. Salcedo, F. C. Ballesteros, A. C. Vilando, M.-C. Lu, *Sep. Purif. Technol.*, 169 (2016) 128–136.
5. J. F. Blais, Z. Djedidi, R. B. Cheikh, R. D. Tyagi, G. Mercier, *Waste Manage.*, 12 (2008) 135–149.
6. D. He, Z. Cao, G. Zhang, L. Zeng, Q. Li, W. Guan, *Chem. pap.*, 73 (2019) 583–589.

7. G. Orhan, C. Arslan, H. Bombach, M. Stelter, *Hydrometallurgy*, 65 (2002) 1–8.
8. N. M. Al-Mansi, N. M. Abdel Monem, *Waste Manage.*, 22 (2002) 85–90.
9. C.-W. Li, J.-H. Yu, Y.-M. Liang, Y.-H. Chou, H.-J. Park, K.-H. Choo, S.-S. Chen, *J. Hazard. Mater.*, 320 (2016) 521–528.
10. V. Coman, B. Robotin, P. Ilea, *Resour. Conserv. Recycl.*, 73 (2013) 229–238.
11. X. Shen, Z. Fang, J. Hu, X. Chen, *Chem. Eng. Sci.*, 280 (2015) 711–719.
12. C. L. Li, H. X. Zhao, T. Tsuru, D. Zhou, M. Matsumura, *J. Memb. Sci.*, 157 (1999) 241–249.
13. I. Giannopoulou, D. Panias, *Miner. Eng.*, 20 (2007) 753–760.
14. I. Giannopoulou, D. Panias, *Hydrometallurgy*, 90 (2008) 137–146.
15. R. Idhayachander, K. Palanivelu, *E-J. of Chem.*, 7 (2010) 1412–1420.
16. J. R. Hernández-Tapia, J. Vazquez-Arenas, I. González, *J. Hazard. Mater.*, 262 (2013) 709–716.
17. A. K. Shukla, S. Venugopalan, B. Hariprakash, *J. Power Sources*, 100 (2001) 125–148.
18. M. Aghazadeh, M. Ghaemi, B. Sabour, S. Dalvand, *J. Solid State Electrochem.*, 18 (2014) 1569–1584.
19. H. B. Li, M. H. Yu, F. X. Wang, P. Liu, Y. Liang, J. Xiao, C. X. Wang, Y. X. Tong, G. W. Yang, *Nat. Commun.*, 4 (2013) 1894.
20. M. Jayalakshmi, M. M. Rao, K.-B. Kim, *Int. J. Electrochem. Sci.*, 1 (2006) 324–333.
21. Y. Ren, L. Wang, Z. Dai, X. Huang, J. Li, N. Chen, J. Gao, H. Zhao, X. Sun, X. He, *Int. J. Electrochem. Sci.*, 7 (2012) 12236–12243.
22. R. Qu, Z. Dai, S. Tang, Z. Zhu, G. M. Haarberg, *Int. J. Electrochem. Sci.*, 12 (2017) 8833–8846.
23. Z. Ge, Y.-Q. Huo, D. Zheng, Q. Zhang, *Int. J. Electrochem. Sci.*, 16 (2021) Article ID: 210541.
24. L. Zheng, C.-R. Zhang, D. Zhao, X. Wang, T.-T. Du, *Int. J. Electrochem. Sci.*, 15 (2020) 5945–5955.
25. H. Cheng, M. Wang, Y. Tang, Y. Sun, Y. Chen, P. Wan, *Int. J. Electrochem. Sci.*, 11 (2016) 6085–6094.
26. Z. Chang, G. Li, Y. Zhao, Y. Ding, J. Chen, *J. Power Sources*, 74 (1998) 252–254.
27. Y. Li, Q. Yang, J. Yao, Z. Zhang, C. Liu, *Ionics*, 16 (2010) 221–225.
28. Y. Li, J. Yao, Y. Zhu, Z. Zou, H. Wang, *J. Power Sources*, 203 (2012) 177–183.
29. B. Shruthi, B. J. Madhu, V. B. Raju, *J. Energy Chem.*, 25 (2016) 41–48.
30. W. Zhang, W. Jiang, L. Yu, Z. Fu, W. Xia, M. Yang, *Int. J. Hydrog. Energy*, 34 (2009) 473–480.
31. C. Miao, Y. Zhu, T. Zhao, X. Jian, W. Li, *Ionics*, 21 (2015) 3201–3208.
32. R. Wang, J. Lang, Y. Liu, Z. Lin, X. Yan, *NPG Asia Mater.*, 7 (2015) e183.
33. X. Zou, J. Hao, Y. Zhou, F. Chen, Q. Hu, B. Xiang, H. Yang, M. Deng, *J. Alloys Compd.*, 855 (2021) 157332.
34. J. H. L. Hadden, M. P. Ryan, D. J. Riley, *Electrochem. Commun.*, 101 (2019) 47–51.
35. Y. Gogotsi, R. M. Penner, *ACS Nano*, 12 (2018) 2081–2083.
36. B. Shruthi, B. J. Madhub, V. B. Rajuc, *J. Energy Chem.*, 25 (2015) 41–48.
37. V. Kovalenko, V. Kotok, *East.-Eur. J. Enterp. Technol.*, 109 (2021) 30–38.
38. V. Kovalenko, V. Kotok, *East.-Eur. J. Enterp. Technol.*, 110 (2021) 45–51.